NACA RM L53A19

NACA

RESEARCH MEMORANDUM

SOME TORSIONAL-DAMPING MEASUREMENTS OF LAMINATED BEAMS AS APPLIED TO THE PROPELLER STALL-FLUTTER PROBLEM

By Atwood R. Heath, Jr.

Langley Aeronautical Laboratory
Langley Field, Va.

NATIONAL ADVISORY COMMITTEE
FOR AERONAUTICS

WASHINGTON

April 29, 1953
Declassified October 12, 1954

NACA RM L53A19

NATIONAL ADVISORY COMMITTEE FOR AERONAUTICS

RESEARCH MEMORANDUM

SOME TORSIONAL-DAMPING MEASUREMENTS OF LAMINATED BEAMS AS APPLIED TO THE PROPELLER STALL-FLUTTER PROBLEM

By Atwood R. Heath, Jr.

SUMMARY

The structural damping, obtained experimentally, in the torsion mode of vibration of a series of untwisted, laminated, thin beams simulating propeller blades is presented in this report. The number of laminations were varied, as well as the bonding material and the method of joining the laminations.

Application of these damping data to the calculation of the minimum flutter speed of thin laminated propeller blades indicates small increases in the minimum flutter speed for models with no bonding material. The use of Cycleweld cement as a bond between laminations increased the damping to the extent that appreciable gains in minimum flutter speed are indicated.

INTRODUCTION

The use of thin supersonic propeller blades has brought about a reduction of the stall-flutter velocity of propellers to the point where stall flutter may be experienced in the take-off range of operating conditions. One promising method for alleviating this condition without changing the primary aerodynamic characteristics is the use of propeller blades with large values of torsional structural damping. Previous research (ref. 1) has shown that the damping of built-up structures in the bending mode can be increased by the use of inserts of various materials between components. In the investigation reported herein, a series of models simulating the dimensions of thin propeller blades have been tested to determine the effect of the number of laminations and the bonding materials on the structural damping in the torsion mode. This work is presented as one direction of research which may ultimately help in providing torsional damping in propeller blades and does not necessarily represent a practical solution to the problem.

SYMBOLS

b	blade semichord, ft
g_α	structural damping coefficient for torsional mode
GJ	torsional stiffness, $lb\text{-}ft^2$
L	blade length, ft
n	number of cycles
V	velocity, ft/sec
α	tip angular deflection, radians
ω_α	first natural torsional frequency, radians/sec

APPARATUS AND TESTING

Apparatus.- The equipment used in these tests is shown with a model in place in figure 1. The model was clamped tightly in the clamping device attached to the upper head, which was in turn securely bolted to one of the wide-flange beams of the building structure. A vane was clamped to the unrestrained lower end of the model in a plane perpendicular to that of the model surface. The vane was designed to facilitate the holding of the model in a twisted position until ready for release and also to offer the minimum amount of surface in the direction of motion. The vane also made possible a release in which only a small amount of bending was introduced into the torsional vibration. An adjustable lever system connected to a solenoid was fastened to the lower head. The hooks of the lever system engaged the vane in the twisted position and were held by the energized solenoid, until the release was made. The components of the optical and recording system (fig. 2) were a line-filament light source, a 12-inch focal-length lens, a front-surface mirror, and a film recorder with timing light. The light-source filament was reflected from the mirror on the model as a vertical image which together with the narrow horizontal slot of the recorder produced a spot on the film.

Models.- The models tested were rectangular in cross section and had a 3-inch chord and 0.0417 thickness ratio regardless of number of laminations. All of the models had a length of 17 inches with the exception of one which had a length of 18 inches. All the models had

a clamped length of 2 inches. The models differed in number of laminations and bonding material and were made of ground tool steel of the following percent composition: carbon, 0.85 - 0.95; silicon, 0.20 - 0.35; manganese, 1.30 - 1.50; and molybdenum, 0.20 - 0.30. Table I lists some properties of the models; figure 3 shows the model cross sections; and a detailed explanation of their construction is as follows:

(1) Model I was composed of solid steel.

(2) Model II was composed of two laminations fastened together in roughly the same manner as brazed hollow-steel propeller blades. On one face of each lamination, a bevel was ground on the leading and trailing edges. The two plates were then joined and silver-soldered together and the model was then ground back to its original chord dimension.

(3) Model III was composed of four laminations, and its construction was the same as that of model II.

(4) Model IV was composed of four laminations; each lamination was attached to an adjacent one by a thin film of soft solder across the entire surface.

(5) Model V was composed of two laminations bonded together with Cycleweld cement, a thermosetting, rubber-plastic-base adhesive, by the CB-4 process. Four force-fit dowels were used to line up the sheets and were located two at the 8.33-percent-chord station and two at the 91.67-percent-chord station.

(6) Model VI was constructed similar to model V with the exception that the dowels were omitted. The leading edge of the model was silver-soldered in the same manner as were models II and III.

(7) Model VI-A was constructed the same as model VI, the only difference being the length, which was 18 inches.

(8) Model VII was similar to model VI but had both leading and trailing edges silver-soldered.

Tests.- All models were twisted to 0.174 radian and released with the resulting torsional vibration being recorded on film. This was repeated until at least two essentially pure torsion records, showing only small amounts of bending vibration, were obtained for each model. Figure 4 shows a typical record of the torsional vibration. During the investigation, several items required additional checking. It was necessary to test the rigidity of the clamping device. Steel wedges were therefore driven between the clamping device and the mounting beam, and vibration records were obtained with model I and compared with previous records for the unwedged clamping device. When model V was being

tested, it was discovered that the second bending mode was interacting with the first torsional mode, so weights were added to the extremities of the vane to separate the frequencies of these two modes. Model I was also tested in this latter configuration and compared with previous tests using no weights on the vane to determine any changes in damping caused by using the weighted vane. It was found impossible by practical means to separate the first torsion and second bending frequencies of model VI sufficiently to give a good record; therefore, a model of longer length, model VI-A, was tested.

Reduction of data.- The torsional structural damping coefficients were evaluated by means of the following equation which has been developed in reference 2, and in which the log decrement δ is equal to πg_α:

$$g_\alpha = -\frac{d\alpha/dn}{\alpha\pi}$$

The damping-coefficient curves were determined from at least two different tests with a maximum relative error involved of about ± 5 percent and with a general relative error of about ± 1 percent. As the damping coefficients were evaluated by determining the slope of the envelope of the decaying vibration, much of the error involved can be attributed to the fairing of the envelope curves as well as the graphical method used for determining the slope of this curve. The absolute value of the damping may also be in error by some indeterminate amount due to the interaction of the model and the vane. Since models I to IV were tested under the same conditions, any error involved should be the same for each one. With weights on the vane for model I, the curve of damping coefficient was displaced upward about 0.0010 from the original. Since model V was tested with the weighted vane, it is seen that the increase in damping coefficient of 0.0010 would amount to 1.5 percent, which is well within the accuracy of determination of this curve. Results of the tests with the wedged clamping device for model I showed a curve that varied only slightly from that of the unwedged model and with no noticeable difference in trend. As the data from tests on model VI-A were repeatable and the damping-coefficient curve fell approximately in the center of a group of curves obtained from model VI, the information from model VI-A is therefore comparable to the models of shorter length.

RESULTS AND DISCUSSION

The data from these tests are shown in figures 5 and 6 where torsional structural damping coefficient is plotted for variation in tip angular deflection. The damping curve for model I agrees at the lower

tip angular deflections with data obtained on a bar of SAE 4130 steel reported in reference 3 but has a slightly lower slope which results in a discrepancy in damping coefficient of 0.001 at the highest tip angular deflections shown. Because of the close agreement of the data, and because the reference data were obtained on a cylindrical bar for which the air damping should be negligible, no correction for air damping is considered to be necessary for the model configuration reported herein.

The structural damping discussed in this report is presented in coefficient form as an equivalent viscous damping and is assumed to be primarily composed of two types of damping, the first being the internal or hysteresis damping of the steel and the bonding materials, and the second, dry-friction damping which is associated with the movement between laminations in models with no bonding material. An inspection of the curves in figures 5 and 6 would lead to the following inferences in regard to the types of damping present for each model. When dry-friction damping is expressed as equivalent viscous damping, as in this report, it varies inversely as the amplitude of vibration when the frequency remains constant. Therefore, as the average slopes of the curves for models II and III are lower than that for model I, it appears that dry-friction damping, as well as internal damping, is present in these two models. The decrease in slope of the damping curves for models II and III from that of model I is about half of that which would be expected from calculations in which the difference between the curves of models II and I and between those of models III and I is assumed to be dry-friction damping. Model III has more sliding surfaces than model II; hence, higher damping values may be expected as shown. The curve for model IV, which has a much higher slope, acts like a homogeneous beam of higher internal-damping capacity than model I, caused no doubt by the soft solder between surfaces.

In figure 6, the damping curve for model VII has a slightly higher slope than model I and varies approximately linearly with deflection, similar to a homogeneous beam of higher internal-damping capacity. Models V and VI-A have damping curves that are probably indicative of a nonhomogeneous structure and are nonlinear throughout the deflection range. As portions of these curves have a lower slope than that of model VII, the addition of dry-friction damping possibly caused by rupture of the Cycleweld bond would seem to be indicated. However, an examination of these models at the end of the tests showed that the bond was still intact. The difference in damping curves between models V and I is assumed to be representative of the internal-damping capacity of Cycleweld. As model VI-A had the leading edge fastened, less working of the Cycleweld is expected, and hence, less damping. As the damping coefficient for model I at the lowest tip angular deflection shown agrees with previously published data (ref. 4), comparisons will be made at this condition.

A method for calculating the stall-flutter parameter $V/b\omega_\alpha$ of thin wings by using the experimental aerodynamic torsional damping-moment coefficients has been presented in reference 5. As the mode of vibration in stall flutter was found to be essentially torsional, the torsional structural damping coefficients reported herein will be applied along with the aerodynamic torsional damping-moment coefficients obtained for the axis of rotation at the 50-percent chord to obtain the minimum flutter parameter. The analysis will be based on the structural properties of an NACA 16-004 airfoil section composed of steel. The minimum flutter parameters calculated from the above are assumed to apply to thin propellers using the 0.8-blade-length station as a reference section, and these parameters are summarized in table I.

The minimum flutter parameter $(V/b\omega_\alpha)_{0.8L}$ is increased from 1.04 for model I to 1.41 for model III, or to 136 percent of that for model I. An increase in the torsional frequency was also obtained (table I) but is not considered significant as a variation was noted for models I to IV.

The increase in damping coefficient for model V over model I at the lowest tip angular deflection, from 0.0012 to 0.0562, is sufficient to raise the minimum flutter parameter to 300 percent of 1.04, or 3.14. As a 5.8-percent reduction in torsional frequency was also obtained, the increase in flutter speed would be less than that shown for the flutter parameter.

Model VI-A, with the leading edge silver-soldered, gave a structural-damping curve that falls between those for models I and V. The increase in damping coefficient over model I from 0.0012 to 0.0240 is sufficient to raise the minimum flutter parameter from 1.04 to 2.44, or to 235 percent of that for model I. As there is no reduction in the torsional frequency of this model, when corrected to a 15-inch free length, the minimum flutter speed will increase directly as the flutter parameter.

Model VII showed an increase in structural damping over model II which had no Cycleweld bond but only equaled that of model III which was discussed above.

The torsional-stiffness factor GJ which normally bears a definite relation to the torsional frequency was determined as a means of verifying the frequency measurements. Models V, VI, and VI-A all showed a similar decrease in torsional stiffness from that of model I, but only model V showed a corresponding decrease in torsional frequency. The fact that the frequency remained constant which is not consistent with the decrease in torsional-stiffness factor would be fortuitous from the flutter standpoint, but the reason for it is not understood. The torsional-stiffness measurements also provided a check on the uniformity

of the models. A variation in stiffness over the length was noted for models V, VI, and VI-A, possibly caused by nonuniformity of the Cycleweld bond; therefore, average values have been tabulated in table I.

CONCLUDING REMARKS

Although the calculated minimum flutter parameters were determined by using aerodynamic damping coefficients taken on thin wings, the magnitude of the indicated gains suggests that appreciable increases in the minimum flutter speed of thin propellers can be expected by such a means. Of the methods of laminations studied, the Cycleweld—silver-solder construction of model VI-A seems to offer the best compromise for the practical construction of a laminated thin propeller blade.

Langley Aeronautical Laboratory,
National Advisory Committee for Aeronautics,
Langley Field, Va.

REFERENCES

1. Cooper, D. H. D.: A Suggested Method of Increasing the Damping of Aircraft Structures. R. & M. No. 2398, British A.R.C., 1950.

2. Schabtach, Carl, and Fehr, R. O.: Measurement of the Damping of Engineering Materials During Flexural Vibration at Elevated Temperatures. Jour. Appl. Mech., vol. 11, no. 2, June 1944, pp. A-86 - A-92.

3. Robertson, J. M., and Yorgiadis, A. J.: Internal Friction in Engineering Materials. Jour. Appl. Mech., vol. 13, no. 3, Sept. 1946, pp. A-173 - A-182.

4. Baker, John E.: The Effects of Various Parameters Including Mach Number on Propeller-Blade Flutter With Emphasis on Stall Flutter. NACA RM L50L12b, 1951.

5. Rainey, A. Gerald: Preliminary Study of Some Factors Which Affect the Stall-Flutter Characteristics of Thin Wings. NACA RM L52D08, 1952.

TABLE I

PROPERTIES OF MODELS TESTED

Model	Free length, in.	Number of laminations	Bonding material	Leading edge silver-soldered	Trailing edge silver-soldered	Torsional frequency, cps (No weights on vane)	Torsional frequency, cps (Weights on vane)	GJ, lb-ft^2	$\left(\frac{V}{b\omega_\alpha}\right)_{0.8L}$
I	15	1	None			92	69	166	1.04
II	15	2	None	Yes	Yes	96	--	180	1.27
III	15	4	None	Yes	Yes	97	--	185	1.41
IV	15	4	Soft solder	No	No	93	--	160	1.06
V	15	2	Cycleweld	No	No	85	65	145	3.14
VI	15	2	Cycleweld	Yes	No	91	--	147	----
VI-A	16	2	Cycleweld	Yes	No	[a]91	--	141	2.44
VII	15	2	Cycleweld	Yes	Yes	92	--	175	1.41

[a]This frequency has been corrected to a free length of 15 inches.

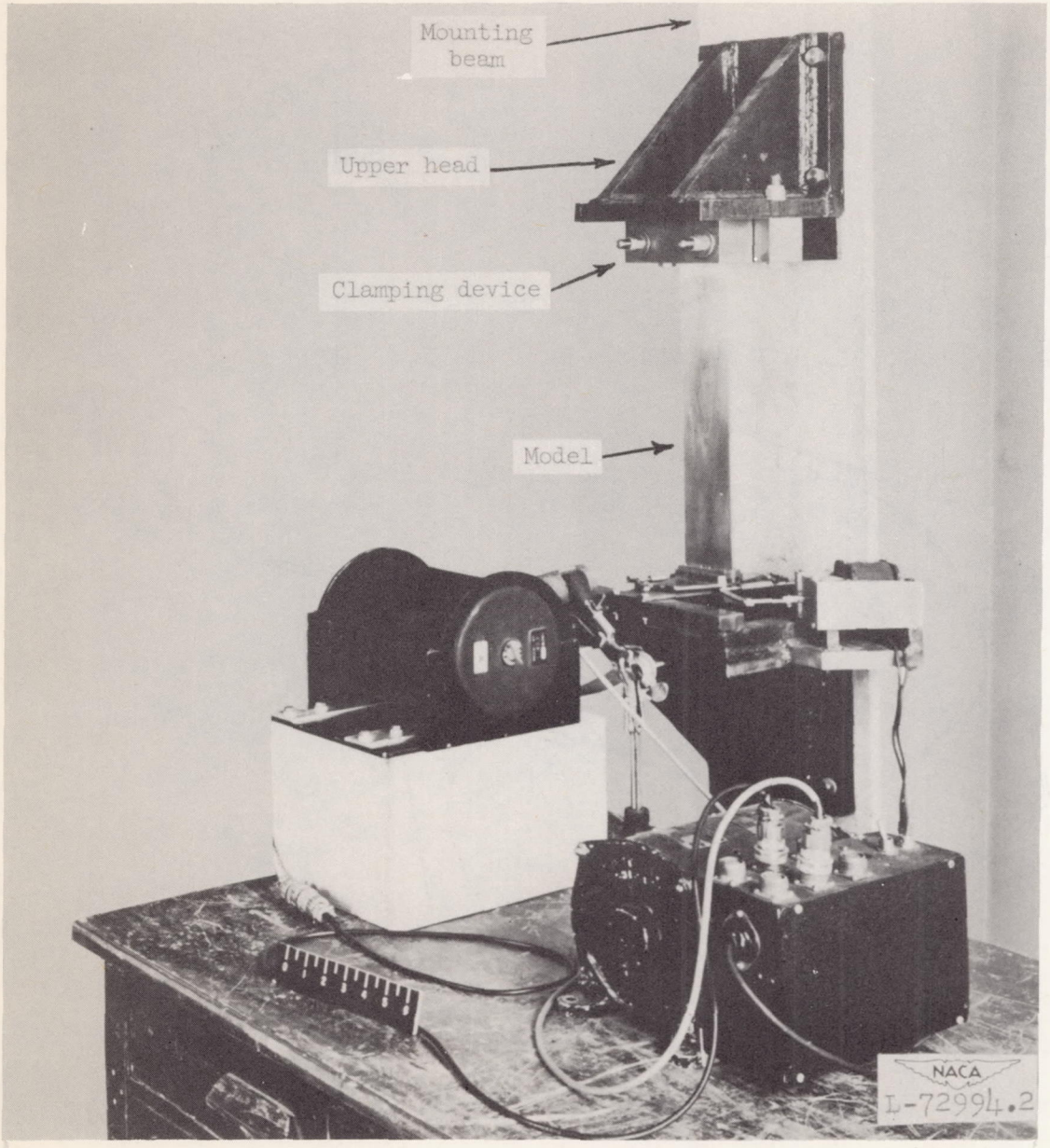

Figure 1.- Test equipment, with model in position, used for obtaining torsional structural damping.

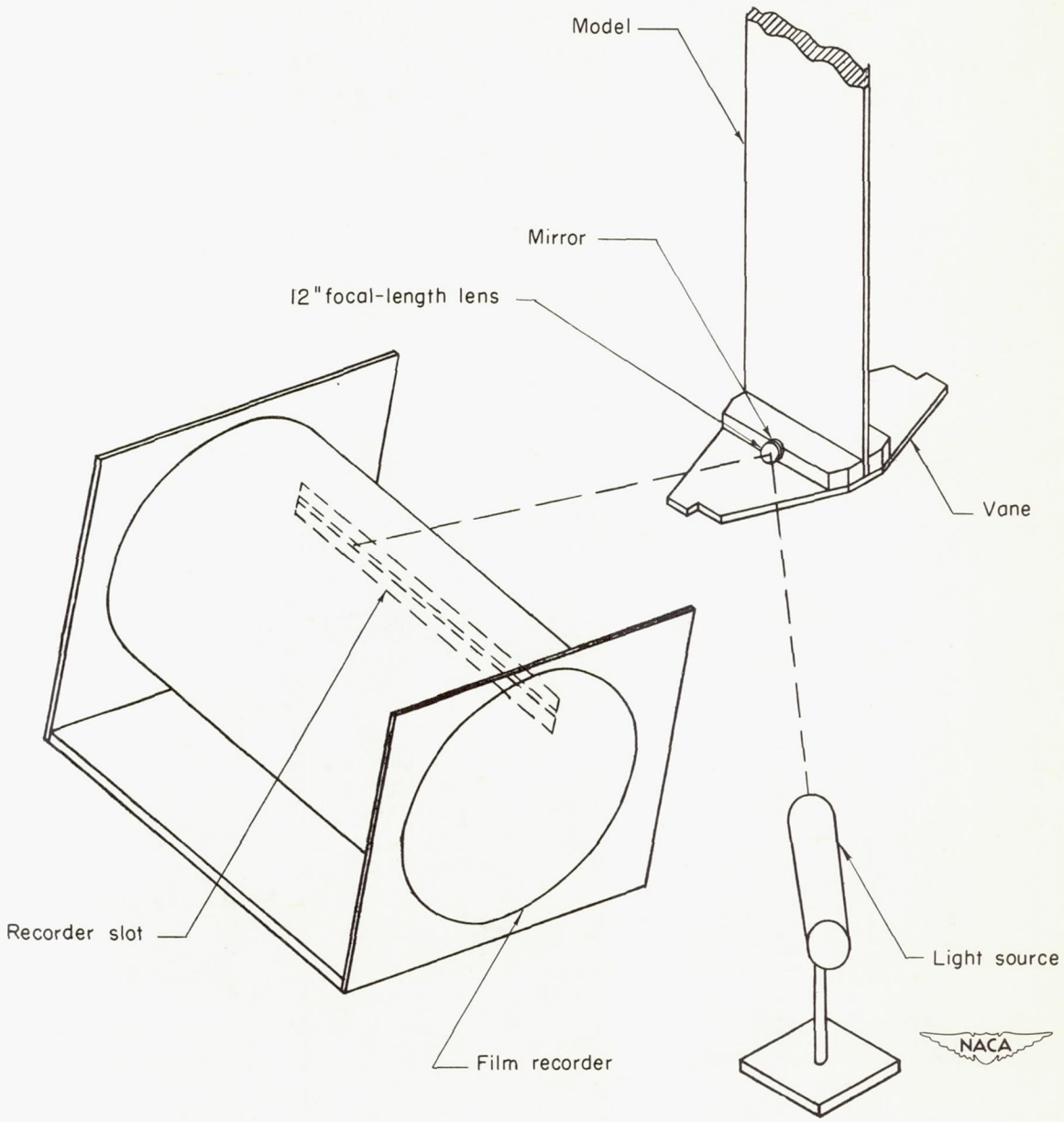

Figure 2.- Schematic drawing of optical system and film recorder.

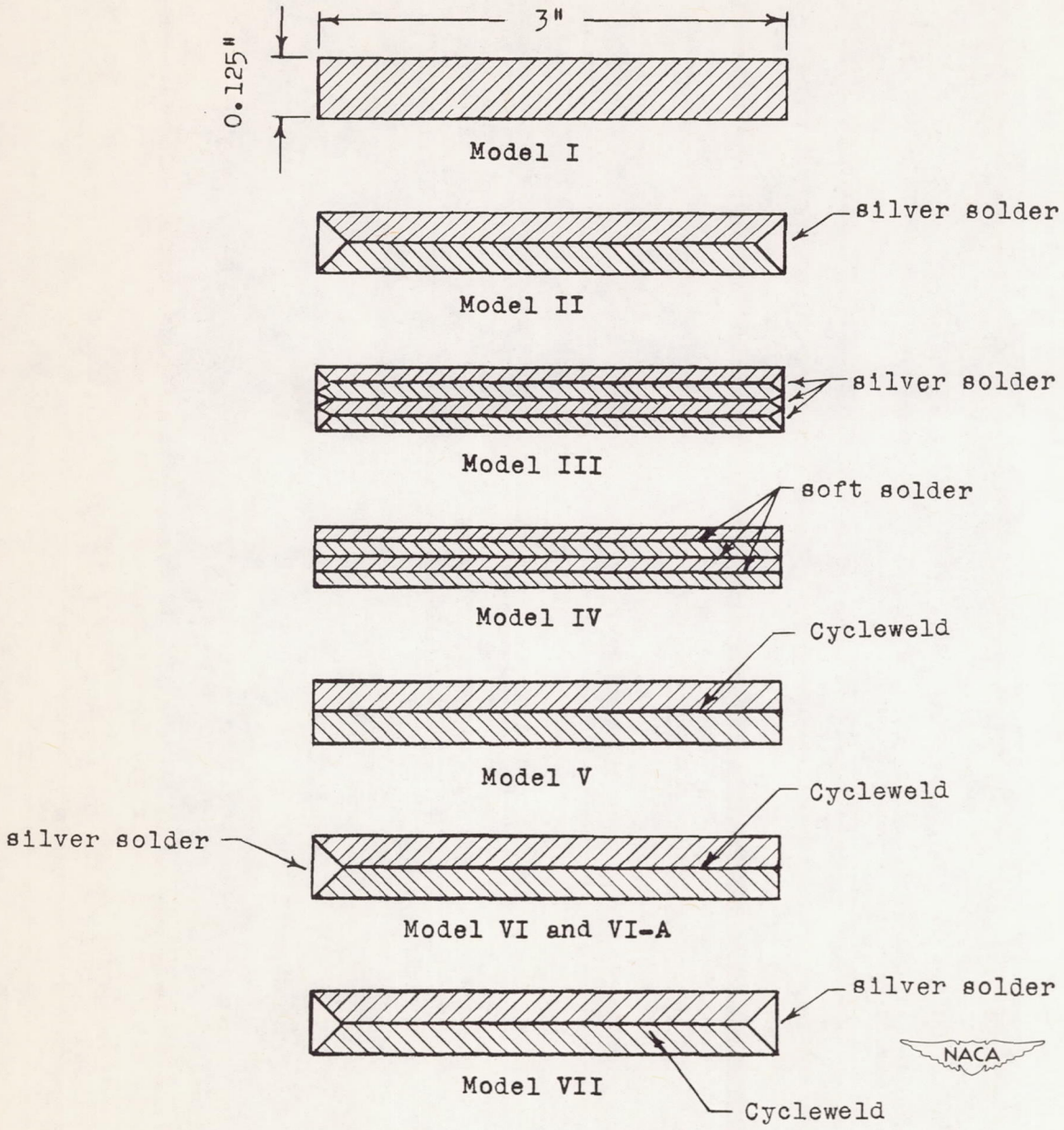

Note: Figures not to scale

Figure 3.- Cross sections of all models.

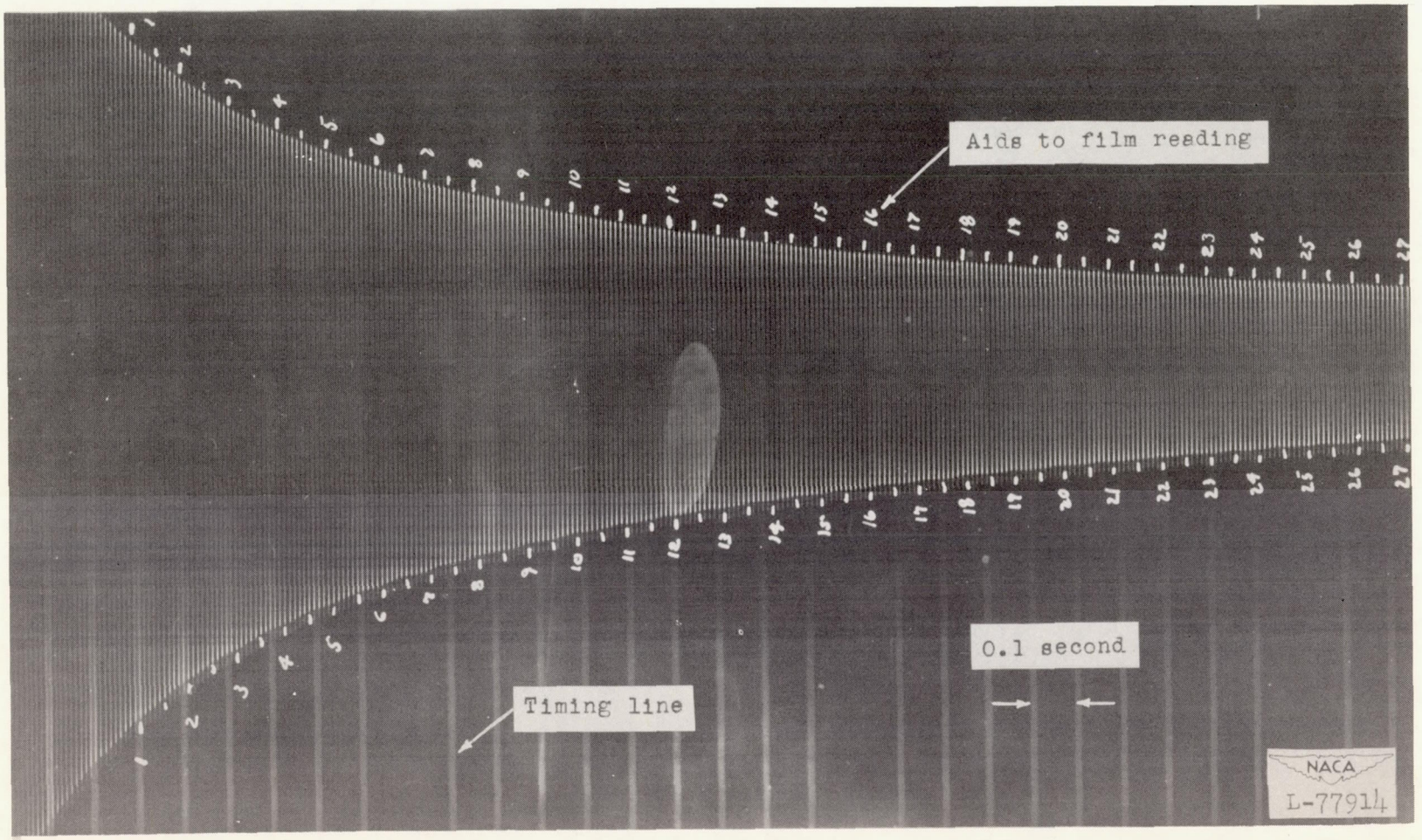

Figure 4.- Typical record of decaying vibration.

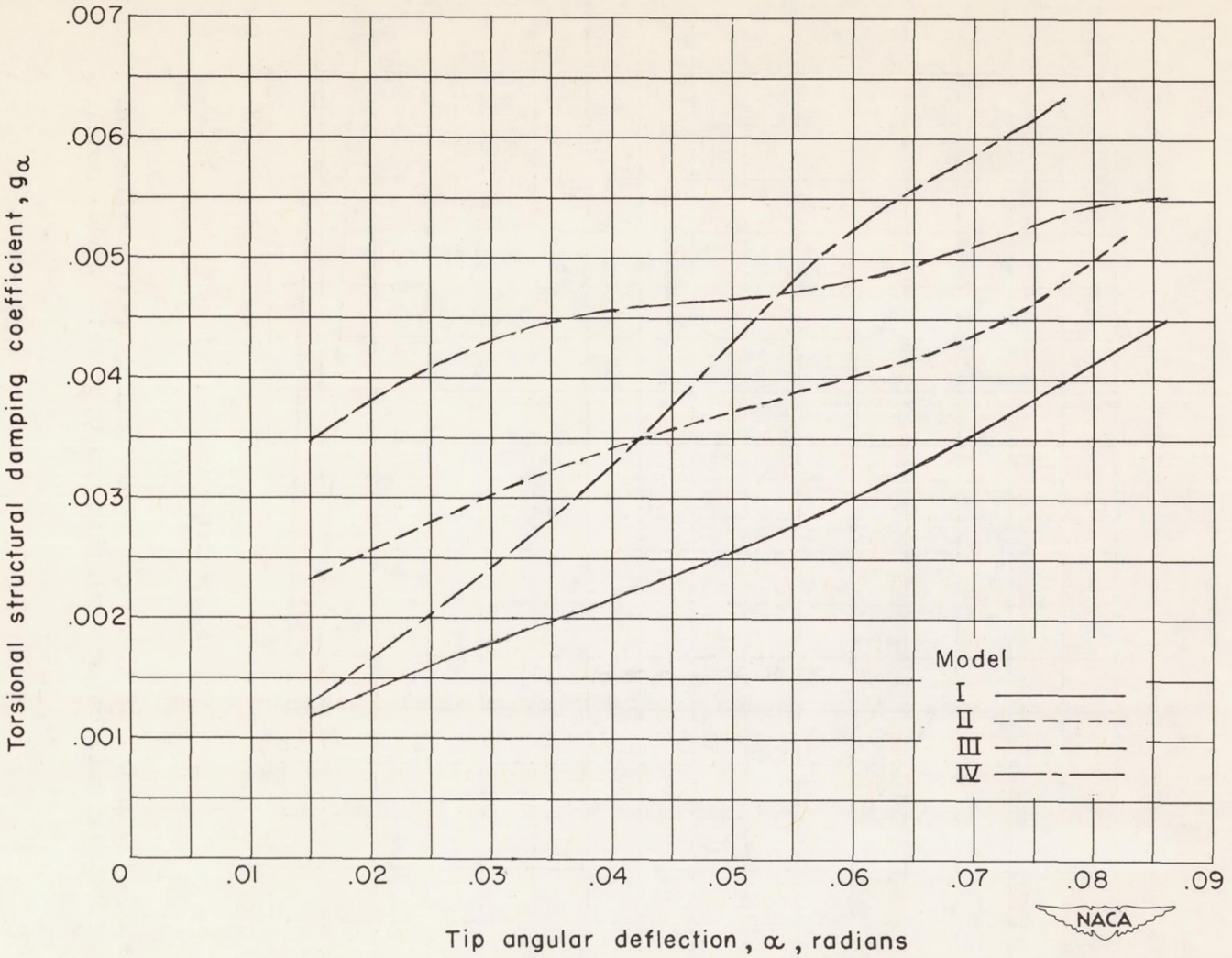

Figure 5.- Variation of torsional structural damping coefficient with tip angular deflection for solid and soldered models.

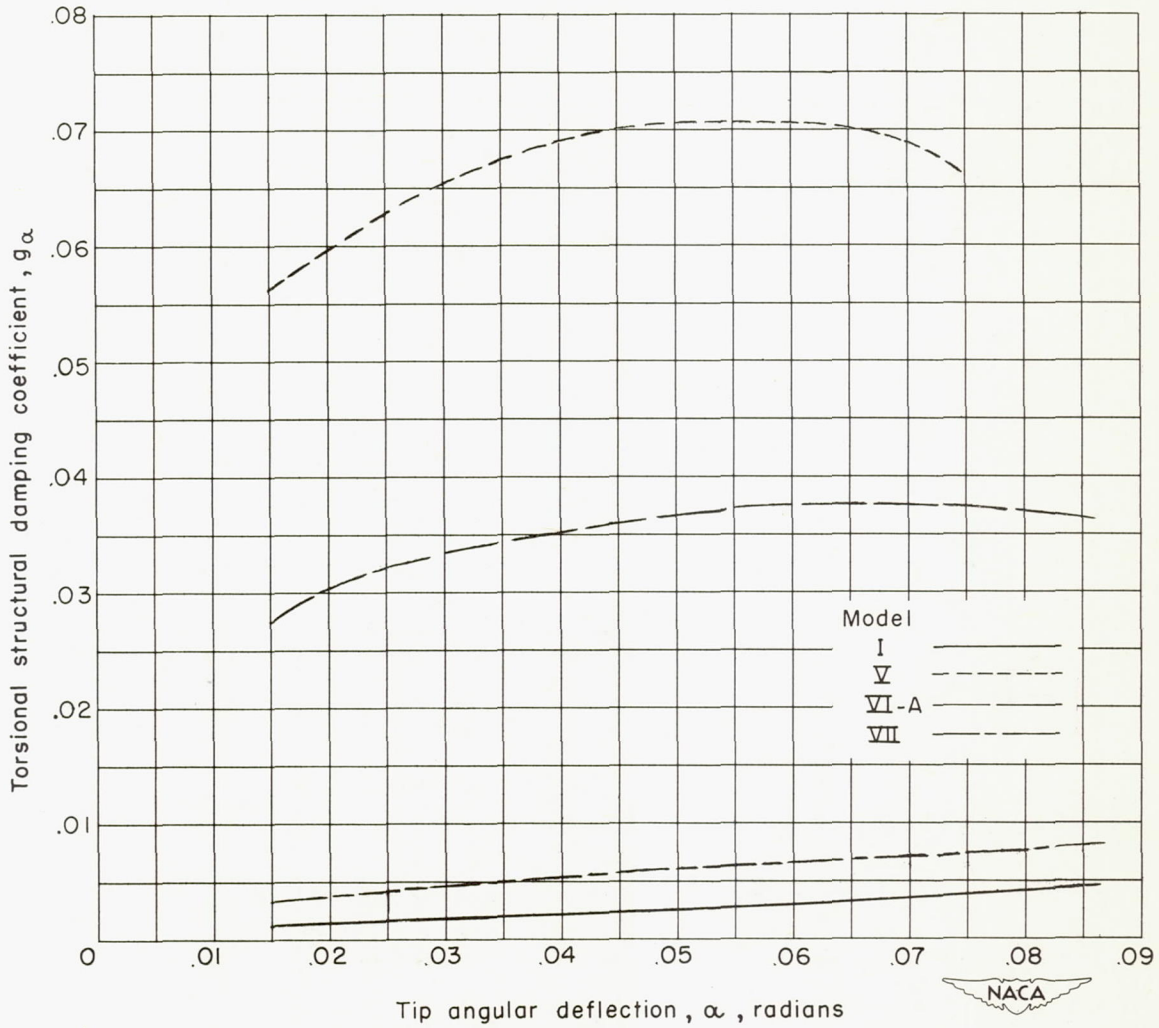

Figure 6.- Variation of torsional structural damping coefficient with tip angular deflection for solid and Cycleweld bonded models.